EFFECT OF MOTOR BRAKING TORQUE ON ENERGY RECOVERY OF REGENERATIVE BRAKING COMBINING SUPERCAPACITOR WITH IGBT CONTROLLER

ẢNH HƯỞNG CỦA MOMENT XOẮN ĐẾN VIỆC THU HỒI NĂNG LƯỢNG CỦA HỆ THỐNG PHANH TÁI SINH KẾT HỢP SIÊU TỤ ĐIỆN VÀ BỘ ĐIỀU KHIỂN IGBT

Pham Quoc Phong[1]*, Bui Phuoc Hai[2]

[1]College of Engineering and Technology, Tra Vinh University, Vietnam
[2]Faculty of Mechanical and Automotive, Nam Can Tho University, Vietnam

*Corresponding author: phongpham@tvu.edu.vn

(Received: January 23, 2026; Revised: May 11, 2026; Accepted: May 20, 2026)

DOI: 10.31130/ud-jst.2026.24(5A).063E

Abstract - Regenerative braking is used on electric vehicles to improve energy efficiency and provide initial partial support for the main braking force. The energy recovered from the regenerative braking system depends on the speed of the vehicle when decelerating and the braking torque of the electric motor. This paper introduces the experimental process and application of Matlab/Simulink to simulate the regenerative braking system on electric vehicles using brushless electric motors combined with supercapacitors and IGBT controllers. The purpose is to investigate the relationship between the motor braking torque and the recovered energy. Then analyze and select appropriate braking methods under specific operating conditions. The results show that the speed before braking and the set braking mode are proportional and decisive factors for the level of recovered energy. The research results can be applied to the design of regenerative braking controllers on electric vehicles or small hybrid vehicles.

Key words - Brushless Direct current Motor (BLDC); Electric Vehicle, IGBT; Regenerative braking; Supercapacitor

Tóm tắt - Hệ thống phanh tái sinh được sử dụng trên xe điện nhằm cải thiện hiệu quả năng lượng và hỗ trợ một phần lực phanh cho hệ thống phanh chính. Năng lượng thu hồi từ hệ thống phanh tái sinh phụ thuộc vào tốc độ của xe khi giảm tốc và moment xoắn của động cơ điện. Bài báo trình bày tiến trình thực nghiệm và ứng dụng Matlab/Simulink để mô phỏng hệ thống phanh tái sinh trên xe điện sử dụng động cơ không chổi than kết hợp với siêu tụ điện và bộ điều khiển IGBT. Mục đích là để nghiên cứu mối quan hệ giữa moment xoắn của động cơ và năng lượng thu hồi được. Sau đó phân tích và lựa chọn các phương pháp phanh phù hợp trong các điều kiện hoạt động cụ thể. Kết quả cho thấy tốc độ trước khi phanh và chế độ phanh được thiết lập là các yếu tố tỷ lệ thuận và quyết định đến mức năng lượng thu hồi. Kết quả nghiên cứu có thể được áp dụng vào thiết kế bộ điều khiển phanh tái sinh trên xe điện hoặc xe hybrid cỡ nhỏ.

Từ khóa - Động cơ điện một chiều không chổi than (BLDC); Xe điện; IGBT; Phanh tái sinh; siêu tụ điện

1. Introduction

Green energy is becoming a global trend. Promoting electric vehicles, combined with renewable energy conversion, is considered a sustainable solution [1]. Recently, regenerative braking has been deployed and extensively researched on electric vehicles using Brushless Direct current Motor (BLDC). Previous studies have analyzed the generator mode on BLDC motors, examining the relationship between output power, rotor speed, and generator losses. The controller utilizes a circuit comprising six or three IGBT/MOSFET switches, which facilitates the recovery of energy to a high level [2, 3]. However, precisely controlling three IGBTs according to the motor's switching time (T) makes the algorithm more complex. To ensure effective and safe braking for vehicles, regenerative braking systems often work in conjunction with conventional friction braking systems. Braking performance affected by the load distribution between the front, rear axles and the braking strategy during vehicle deceleration in regenerator mode [4]. The research underscores the necessity for improved braking strategies and emphasizes their urgency. Based on investigations, regenerative braking significantly influences vehicle stability during braking, cornering, or various driving conditions [5]. Proactive control of the regenerative braking force, specifically the ability to regulate the braking torque of the electric motor during deceleration, warrants further in-depth study [6].

During the process of receiving voltage, the storage will act as a load, creating a braking torque to help the motor decelerate. If using battery packs with fast charging capability, the braking torque generated by the motor will be greater. Previous studies have shown that electric drive systems are supplemented with auxiliary energy storage units, specialized to store the energy recovered during braking, called Hybrid Energy Storage System - HESS. Because of the limited energy density, the supercapacitor is only suitable for short-term energy storage, the energy to ensure the essential operation of the vehicle is still provided by the battery [7-9]. However, several studies have focused on optimizing Hybrid Energy Storage Systems (HESS) for electric vehicles and micro-electric vehicles, combining Li-ion batteries and supercapacitors [10]. This solution aims to leverage the high energy density of batteries and high-power output of the supercapacitors to improve operational efficiency and extend the lifespan of the power source. The authors proposed using intelligent algorithms such as swarm optimization (PSO) and genetic algorithms (GA) to control the PID controller and fuzzy logic, helping to distribute current efficiently between the two storage sources. Integrating supercapacitors is key to improving economic efficiency and promoting the adoption of electric vehicles in urban areas. HESS systems on electric vehicles are shown in Figure 1. Therefore, to analyse and compare the impact of braking torque and give a reasonable control algorithm, experiments and simulations will use supercapacitors.

While driving, electric vehicles move through different routes such as highways and inner-city roads [11]. When encountering dangerous situations that require braking or slowing down, the factors affecting the efficiency of regenerative energy are the state of charge of the battery pack (SoC), the speed at the time of starting to decelerate, the braking intensity (i.e., the braking torque generated by the motor), pedal travel, pedal travel change rate, and steering angle. In addition, the braking control strategies also have an influence [12-14].

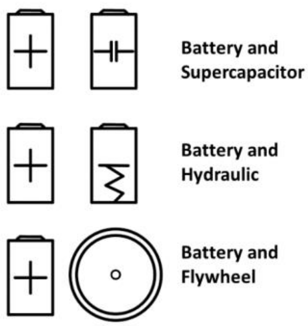

Figure 1. *Typical HESS systems on electric vehicles*

Accordingly, the general situation of recent studies shows that the research trend in this field is focusing on the distribution of braking force. To do that, the requirement is to control the braking torque generated by the electric motor, thereby creating a basis for studying the coordination algorithm with the mechanical brake. In this study, to simplify the control, IGBT switch is used to replace the 6 switches on the voltage divider. In addition, to control the braking torque and analyze the recovered voltage at different braking torques along with the energy recovery efficiency of the supercapacitor in single-pedal mode, a control circuit using IGBT power lock-up and an experiment were built. Simulations were also performed on Matlab/Simulink to analyze and record the results. This paper proposes a 4-mode braking strategy that can be actively selected by the driver depending on driving conditions for a regenerative braking system on small electric vehicles. Using the STM32 microcontroller and various electronic components, a test control circuit is fabricated, which can be flexibly used for different regenerative braking systems.

2. Modeling development

2.1. Matlab/Simulink model

The BLDC motor can maximize energy recovery during braking and maintain smoothness when the vehicle decelerates [15]. The simulation of a BLDC motor in Matlab/Simulink is done using the Permanent Magnet Synchronous Machine block because it has trapezoidal reverse emf, similar to the characteristics of a BLDC motor in regenerative braking mode. The energy storage system on electric vehicles usually uses lithium batteries, or some vehicles use lead-acid batteries, both of which provide direct current (DC). The BLDC motors used on vehicles are three-phase AC motors. This type of motor can recover renewable energy, which needs to be converted from three-phase AC to DC. There are many methods for rectifying three-phase current to DC current. Non-isolated topologies include: buck, boost, buck–boost, switched capacitor, interleaved structures, and multilevel stages [16]. Among these methods, the diode bridge rectifier is considered the most basic method and has a simple design, and is easy to implement for this process. Therefore, in the scope of this paper, a diode bridge will be used to rectify the current from the BLDC motor during regenerative braking. The voltage recovery will be performed by the supercapacitor block because it has the characteristic of absorbing current quickly. In order to investigate the relationship between the braking torque of the BLDC motor and the recovery voltage. The simulation of the supercapacitor in Matlab/Simulink is performed through the Supercapacitor block in the Simscape library.

According to the single-pedal principle, braking force is handled by the electric motor when the pedal is lifted. When accelerating, the pedal is pressed down again. The simulation model used the motor speed and PWM pulses to control the semiconductor switches according to each braking mode. The speed and stopping time of the motor were measured and recorded during the experiment. PWM pulses were provided by the microcontroller. Therefore, the speed parameters and PWM pulses in the simulation will be coded and data will be entered into Simulink through the Workspace block. After completing the assembly of the component blocks, the simulation model will be built with the structure as shown in Figure 2. Parameters of the component blocks in the simulation are presented in Table 1.

Table 1. *Simulation Parameters in Matlab/Simulink*

Module	Parameter	Value
BLDC Motor	Number of phases	3
	Back EMF waveform	Trapezoidal
	Mechanical Input	ω
	Stator phase resistance Rs	0.0485
	Stator phase inductance Ls	8.5e-3
	Flux linkage	0.1194
	Back EMF flat area	120
Capacitor	Rated capacitance	6.66
	Equivalent DC series Resist	8.9e-3
	Rated voltage	64.8
	Number of series Capacitors	24
	Initial voltage	12.50
Diode	Resistance Ron	0.001
	Forward voltage Vf	0.8
	Snubber resistance Rs	500
IGBT	Resistance Ron	0.001
	Forward voltage Vf	1.85
	Snubber resistance Rs	1e5

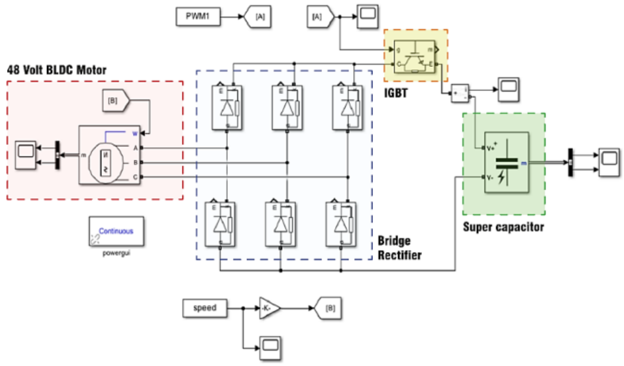

Figure 2. *The simulation model of the regenerative braking system*

2.2. Experimental model

To verify simulation results, an experiment was implemented. The 750W BLDC motor is combined with a flywheel to simulate a small electric vehicle of about 200 kg in the process of deceleration. The experimental diagram is shown in Figure 3.

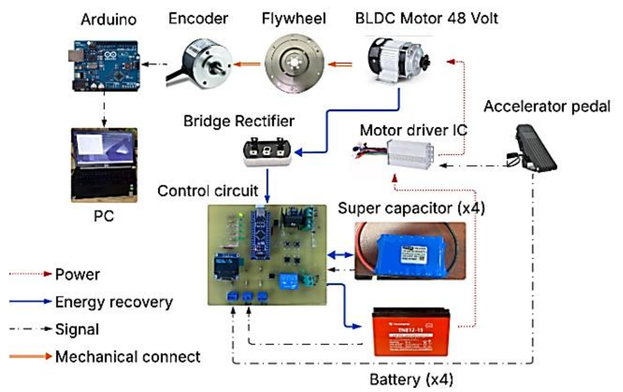

Figure 3. *Diagram of a regenerative braking system*

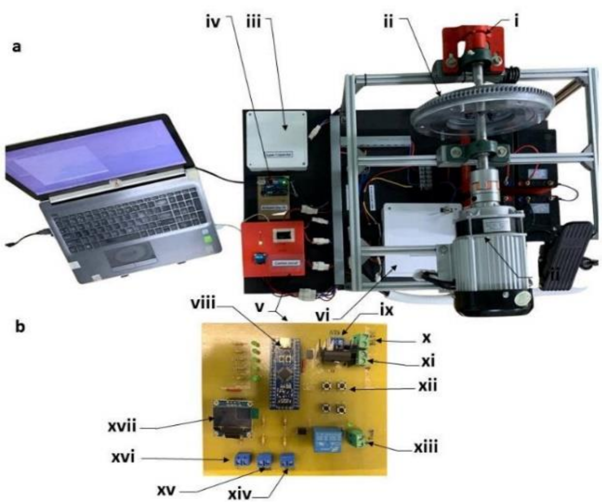

Figure 4. *Experimental setup for regenerative braking process*

(a) Experimental overview model with (i) Encoder, (ii) Flywheel, (iii) supercapacitor, (iv) Arduino, (v) Control circuit, (vi) Control IC, (vii) BLDC; (b) Control circuit with (viii) STM32F103CBT6, (ix) 12V port, (x) Voltage receiving port from rectifier bridge, (xi) Charging port for supercapacitor, (xii) Mode selection button, (xiii) Battery charging port, (xiv) Supercapacitor voltage reading port, (xv) Battery voltage reading port, (xvi) Accelerator pedal signal port and (xvii) Display screen

Figure 4 shows the experimental model. Based on the input signal from the push button, the microcontroller will automatically change the frequency or width of the PWM pulse to achieve the desired control effect.

The motor speed is measured using an Arduino Uno R3 microcontroller, and the speed value is sent directly to the computer via the serial port for data storage. The measurement resolution depends on the pulse-counting method and sampling interval, with an estimated accuracy of approximately ±1–2%. The voltage measurement of the battery and supercapacitor, and the width of the PWM is performed through the STM32F103CBT6 microcontroller, the measured value is displayed through the OLED screen designed to be mounted on the circuit, and the Oscilloscope Hantek6022BE 20MHz. The accuracy of Hantek6022BE is ±3%, the sampling rate is 48 ms/s, and the default test pulse on board is 1kHz 2V pp (square wave). Calibration is performed before measurement to ensure accuracy. Each experimental condition was repeated three times, and the average value was used for analysis in order to improve measurement reliability and reduce random errors. However, several factors can cause discrepancies between experimental and simulation results, including mechanical and electrical losses, measurement noise, and differences between the assumed parameters in the simulation and the real hardware (e.g., resistance and inductance).

3. Results and discussion

Simulation on Matlab/Simulink is performed based on experimental parameters. In which the motor speed range is kept at the maximum level, and 4 braking modes provide 4 pulse widths from 0 to 100%. In experimental conditions, when the car is running, the accelerator and brake pedals are released, the car's speed will tend to decrease gradually until it stops completely. Experiments and simulations will be performed with the following parameters:

- Case (i): 535 RPM, PWM = 0%.
- Case (ii): 535 RPM, PWM = 25%.
- Case (iii) : 535 RPM, PWM = 75%.
- Case (iv) : 535 RPM, PWM = 100%.

3.1. Analysis of case (i)

Figure 5 illustrates the electromagnetic torque generated by BLDC, with the x-axis depicting time in seconds and the y-axis representing electromagnetic torque (N*m). It can be seen Te with slight oscillation in the initial stage due to the motor being in the transition phase from motor mode to generator mode. However, the oscillation value is very small. The oscillation level is around -1N*m for a very short period of time, less than 0.001 seconds. This is shown more clearly in Figure 6, the braking force in this case will not be generated by the electric motor.

If the vehicle is moving in unsafe road conditions or when cornering, this case is recommended because it does not cause the wheels to suddenly lock up, leading to dangerous situations. However, the problem is to calculate the recovery voltage power and the rated power of the IGBT to ensure the safety of the circuit.

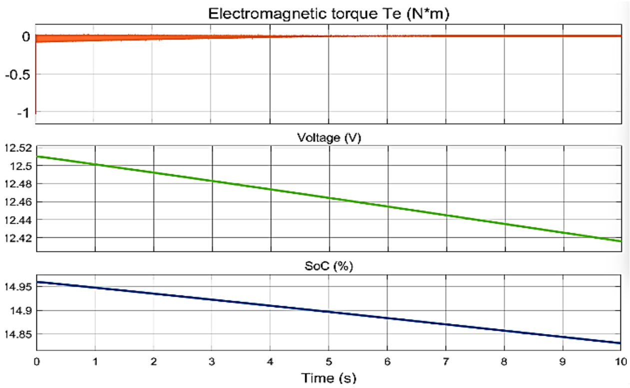

Figure 5. *Braking torque generated by the motor, voltage and charging factor of the supercapacitor in case (i)*

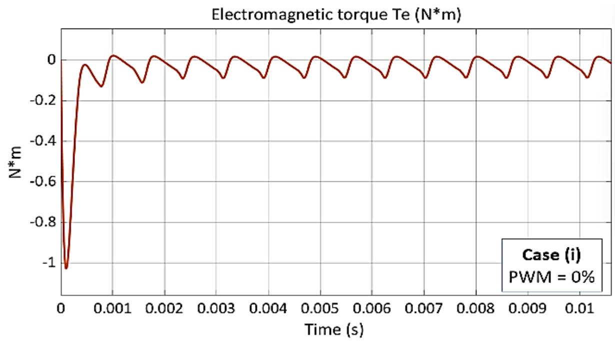

Figure 6. *Electromagnetic torque in case (i)*

3.2. Analysis of case (ii)

Figure 7 shows the value of Electromagnetic torque (Te), voltage (V), and state of charge (SoC) in this case. The figure is divided into two stages, a and b. According to stage a, the Te value fluctuates from 1.5N*m to -15N*m in the first 1 second after deceleration. The voltage and state of charge of the supercapacitor also increase rapidly. Specifically, the voltage increases from 12.5V to more than 13.2V, the state of charge also increases from 15% to about 15.7%. This braking torque will cause the motor speed to decrease, but the level of reduction is low, so in the later stage (stage b), the speed range is still at a level that can generate voltage. Then, the voltage continues to be recharged into the supercapacitor according to each IGBT open cycle in the following seconds. After stage b, the vehicle will completely lose its braking force because the energy is no longer recharged. At this time, the vehicle will drift by inertia.

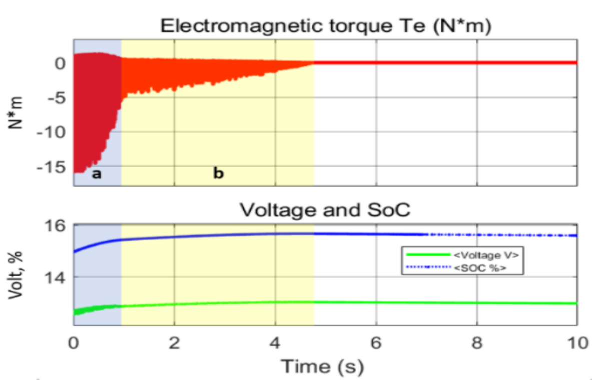

Figure 7. *Braking torque generated by the motor, voltage, and charging factor of the supercapacitor in case (ii)*

3.3. Analysis of case (iii) and case (iv)

The electromagnetic torque in Figure 8 is divided into 4 small stages. Stages a and b are where the electric motor creates the largest braking torque, which can cause the motor to stop suddenly. Stages b and c are where the motor speed has decreased, but can still create energy and braking force. Stage d is where the motor speed is no longer large enough to create energy.

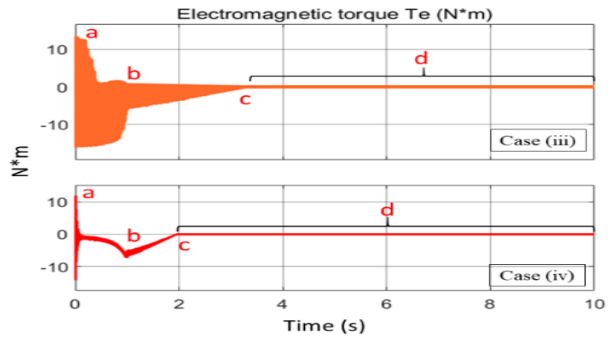

Figure 8. *Braking torque generated by the motor in case (iii) and case (iv)*

Case 3, in stage a (about the first 0.5 seconds), due to the high speed of the motor, the voltage generated is large, so the Electromagnetic torque (Te) has an amplitude ranging from 14N*m to -15N*m. At this time, the braking torque generated by the motor is the largest. However, because the IGBT only opens 75% of the cycle compared to the total time, the braking torque received by the vehicle is only about 75%, and there is still a ripple phenomenon due to the IGBT's opening and closing cycle. Then, in phase b to phase c, motor speed decreased but was still maintained at the speed range that can generate voltage, the braking torque is still generated, compared to phase a, it decreased significantly. The amplitude of the electromagnetic torque oscillation is between 2N*m and -15N*m in phase b, then gradually decreases to 0N*m in phase c. In stage d, this is the stage where the electric motor can no longer generate braking force because the speed has decreased to a very low level. The total time from the start of deceleration until the motor can no longer generate braking torque in this case is about 3.84 seconds. Figure 9 presents the voltage and speed of the motor in case (iv). At the 2-second mark after deceleration, the voltage of the supercapacitor reached nearly 16V. However, the BLDC speed had decreased to a low level, and no voltage could be generated, so the supercapacitor voltage showed no signs of increase.

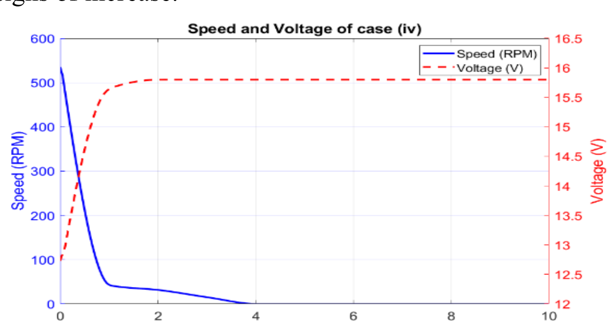

Figure 9. *Voltage and speed of motor in case (iv)*

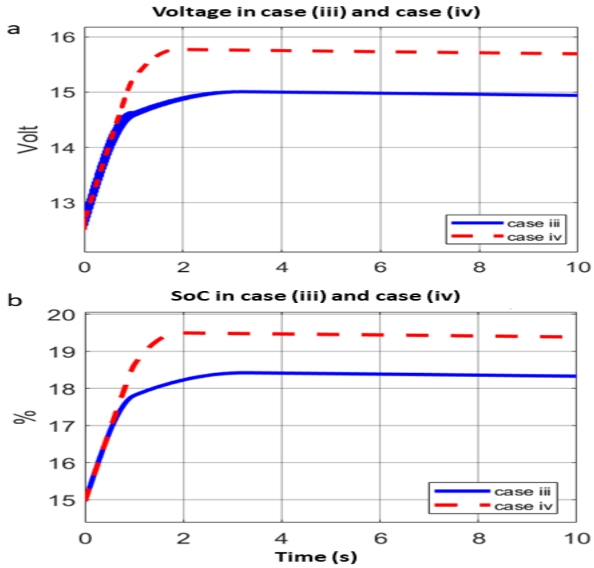

Figure 10. *Voltage and state of charge of Supercapacitor in case (iii) and case (iv): a. Voltage, b. State of charge*

Figure 10 depicts the voltage parameters and state of charge (SoC) value of the supercapacitor in cases (iii) and (iv) with Figure 10.a shows the voltage, and Figure 10.b shows the SoC value. To evaluate the performance of a regenerative braking system, the energy recovered and stored by the supercapacitor will be calculated as follows Eq. (1):

$$E = \frac{1}{2}C(V_2^2 - V_1^2) \quad (1)$$

Where C is the capacitance, and V_1, V_2 are voltages. In case (iv), the supercapacitor voltage increases from 12.5V to approximately 16V at a capacitance of 6.66F, yielding an energy recovery of approximately 330 J. The initial kinetic energy of the system, equivalent to the mass of the car of about 200kg, can be calculated using the following formula Eq. (2):

$$E_k = \frac{1}{2}mv^2 \quad (2)$$

Based on the given parameters, the initial kinetic energy is approximately 3 kJ. Therefore, the recovered energy accounts for about 10% of the initial kinetic energy. This is likely due to the remaining energy being dissipated through various loss mechanisms, including copper losses in the stator windings, power electronic losses in diode bridges or switching devices, and mechanical losses such as friction and air resistance, so only a portion of the kinetic energy can be recovered. To compare the regenerative braking under different braking modes, the recovered energy and energy recovery efficiency were calculated for all cases. The recovered energy stored in the supercapacitor was determined based on the measured voltage variation.

The results (Table 2, 3) demonstrate that the recovered energy increases proportionally with the PWM duty cycle and braking torque. Case (iv) achieved the highest energy recovery efficiency of approximately 10%, while case (i) showed no energy recovery because the regenerative braking function was disabled. These results confirm that increasing the regenerative braking torque can significantly improve the amount of recovered energy.

Table 2. *Voltage, ampe and deceleration time*

Case	Deceleration time (s)	Ampe (A)	Initial Voltage (V)	Voltage after deceleration (V)
Case (i)	7.03	0	12.5	12.5
Case (ii)	5.09	2.9	12.5	13.4
Case (iii)	4.04	3.26	12.5	14.4
Case (iv)	3.89	3.28	12.5	15.3

Table 3. *Regenerative energy recovery*

Case	Voltage (V)	Energy (J)	Efficiency (%)
Case (i)	12.5	0	0
Case (ii)	13.4	82	2.7
Case (iii)	14.4	195	6.5
Case (iv)	15.3	330	10.0

3.4. Comparing simulation and experimental results

Table 4 compares the experimental and simulated voltage results for all four cases. The experimental results show good agreement with the simulation, with deviations below 10%. To evaluate the agreement between the simulation and experiment, the error between the simulated and measured voltage was calculated using Eq. (3):

$$Er(\%) = \frac{|V_{sim} - V_{exp}|}{V_{exp}} * 100 \quad (3)$$

Where V_{sim} is simulated voltage and V_{exp} is experimental voltage.

Table 4. *Voltage of simulation and experiment*

Case	Simulation	Experiment	Er (%)
Case (i)	12.5	12.5	0
Case (ii)	13.2	13.4	1.49
Case (iii)	14.9	14.4	3.47
Case (iv)	15.8	15.3	3.27

Errors for cases are presented in Table 4. The results indicate that the maximum deviation between simulation and experimental data is below 4%, demonstrating good agreement and validating the proposed simulation model. The small discrepancies are mainly caused by practical losses in the experimental system, including winding resistance, switching losses of the IGBT, diode bridge losses, friction losses of the flywheel system, and measurement noise from the sensing devices.

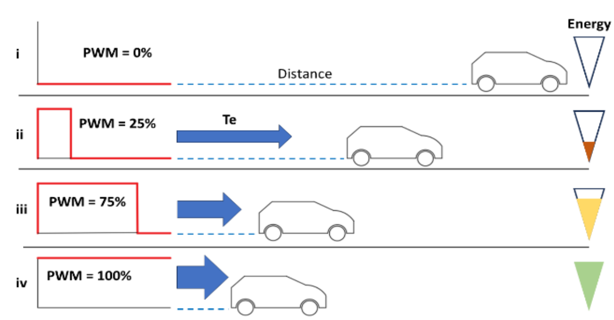

Figure 11. *Experiment and simulation results in four cases*

Figure 11 illustrates the overview of the experiment and simulation results of cases (i), (ii), (iii), and (iv). Accordingly, in case (i), the motor has no braking torque, so the stopping distance will be the longest, and the energy recovery is nonexistent. The shortest stopping distance is in case (iv) when the braking torque is the largest and the energy recovery is the highest compared to the other cases.

3.5. Some limitations of the study

In this study, the accelerator pedal signal is used as the main signal for the algorithm. For vehicles used for a long time, the accelerator pedal will have a reduced lifespan, the microcontroller receives a signal that is disturbed by the accelerator pedal, leading to the operating modes in the control circuit no longer being accurate. For example, in the case of a light force on the accelerator pedal, the electric motor will operate, but the wrong signal will make the microcontroller misunderstand that the electric motor is not yet operating or is decelerating, and the PWM will be supplied. When the electric motor is operating, the 3-phase wires of the motor take power from the control IC, so the voltage at this time on the 3-phase wires of the motor will be close to the voltage of the battery source on the vehicle. Because the PWM is being supplied, the IGBT will open the charging path to the supercapacitor, and the vehicle will fall into a state of running and charging. This is extremely harmful to the electric motor and the supercapacitor. First, the supercapacitor will be overcharged. Second, since the supercapacitor is being charged, a braking force is also created on the electric motor, which restrains the rotation of the electric motor.

The PWM modes on the control circuit also need to be manually selected by the driver, which can be inconvenient when the driver always has to calculate and choose which mode to use while moving, making the driver easily lose concentration. However, this is also beneficial if the driver wants to be more independent in recovering energy, extending the vehicle's range, and ignoring the smoothness when driving.

4. Conclusion

The paper presents the experimental construction and Matlab/Simulink simulation of the regenerative braking system on an electric vehicle using a BLDC motor combined with supercapacitors. The relationship between the braking torque of the BLDC motor and the recovered regenerative energy, along with the selection of braking mode, has been explained. Depending on the traffic conditions and the remaining capacity of the vehicle's battery, the driver can flexibly switch between modes to balance the smoothness and recovered energy while driving. To improve efficiency, the study proposes to integrate the experimental controller on a real electric vehicle to test the circuit's performance. The model can be applied to the development of an effective regenerative braking controller, suitable for small electric vehicles and hybrid vehicles.

REFERENCES

[1] R. R. Timilsina, J. Zhang, D. B. Rahut, K. Patradool, and T. Sonobe, "Global drive toward net-zero emissions and sustainability via electric vehicles: an integrative critical review", *Energy, Ecology and Environment*, vol. 10, pp. 125–144, 2025. doi: 10.1007/s40974-024-00351-7.

[2] J. A. Ruz-Hernandez, L. Djilali, M. A. Ruz Canul, M. Boukhnifer, and E. N. Sanchez, "Neural Inverse Optimal Control of a Regenerative Braking System for Electric Vehicles", *Energies*, vol. 15, no. 23, 2022. doi: 10.3390/en15238975.

[3] P. Stawczyk, "Costless Improvement of Converter Efficiency in a Regenerative Braking System with a Brushless DC Machine", *Electronics*, vol. 14, 2025. doi: 10.3390/electronics14122390.

[4] N. T. Anh, C.-K. Chen, and X. Liu, "An Efficient Regenerative Braking System for Electric Vehicles Based on a Fuzzy Control Strategy", *Vehicles*, vol. 6, no. 3, pp. 1496–1512, 2024. doi: 10.3390/vehicles6030071.

[5] R. Levickas and V. Žuraulis, "Stability Issues of Rear–Wheel–Drive Electric Vehicle During Regenerative Braking", *Applied Sciences*, vol. 15, no. 20, 2025. doi: 10.3390/app152010926.

[6] V. P. Nguyen, V. N. Tran, và M. D. Le, "Experimental study on HEV series truck model", *The University of Danang - Journal of Science and Technology,* vol. 23, no. 12, pp. 39-44, 2025, doi: 10.31130/ud-jst.2025.23(12).381E.

[7] E. M. Szumska, "Regenerative Braking Systems in Electric Vehicles: A Comprehensive Review of Design, Control Strategies, and Efficiency Challenges", *Energies*, vol. 18, no. 10, 2025. doi: 10.3390/en18102422.

[8] M. Ehsani, Y. Gao, S. Longo, and K. Ebrahimi, *Modern Electric, Hybrid Electric, and Fuel Cell Vehicles,* 3rd edition. Boca Raton, FL, USA: CRC Press, 2018.

[9] S. M. Michael, B. Mtengi, S. R. S. Prabaharan, A. M. Zungeru, and J. G. Ambafi, "Design of Regenerative Braking System and Energy Storage with Supercapacitors as Energy Buffers", *International Journal of Electrical and Computer Engineering Systems*, vol. 15, no. 4, 2024.

[10] S. Harippriya, S. Jayanthy, and E. E. Vigneswaran, "Design and Implementation of Hybrid Energy Storage System Integrating Lithium-ion Battery and Wind Turbine", *IOP Conf. Ser.: Mater. Sci. Eng.,* vol. 1291, no. 1, 2023. doi: 10.1088/1757-899X/1291/1/012042.

[11] I. Pielecha, W. Cieślik, and K. Fluder, "Analysis of energy management strategies for hybrid electric vehicles in urban driving conditions", *Combustion Engines*, vol. 173, no. 2, pp. 14–18, 2018. doi: 10.19206/CE-2018-203.

[12] N. Hannan, S. K. Shib, A. Shufian, M. A. Islam, S. M. M. I. Sharan, and A. D. Gupta, "Advanced regenerative braking system for EVs: Leveraging BLDC-supercapacitor technologies for optimized energy recovery, economic viability, and maintenance strategies", *Future Batteries*, vol. 7, no. 100103, 2025. doi: 10.1016/j.fub.2025.100103.

[13] Q. P. Pham, T. E. Nguyen Van, and P. H. Bui, "Investigation of regenerative braking torque of electric vehicles using BLDC machines with PWM controlled IGBT," in *Proceedings of the 8th International Conference on Research in Engineering and Technology (RET 2025)*, pp. 247–251, 2025.

[14] P. H. Bui, C. T. Le, T. T. Dang, and Q. P. Pham, "Predictive mode of energy recovery in regenerative braking system of electric vehicles," *Journal of Science and Development Economics*, no. 1, pp. 48–54, 2026, doi: 10.64632/jsde.eng.1.2026.713.

[15] W. Chen, J. Wu, X. Li, and C. Li, "Overvoltage Avoidance Control Strategy for Braking Process of Brushless DC Motor Drives with Small DC-Link Capacitance", *Actuators*, vol. 13, no. 5, 2024. doi: 10.3390/act13050185.

[16] H. Naseem and J. K. Seok, "Recent Advances in Bidirectional Converters and Regenerative Braking Systems in Electric Vehicles", *Actuators*, vol. 14, no. 347, 2025. doi: 10.3390/act14070347.